Split EPR Signals from Photosystem II Are Modified by Methanol, Reflecting S State-Dependent Binding and Alterations in the Magnetic Coupling in the $CaMn_4$ Cluster†

Ji-Hu Su,‡ Kajsa G. V. Havelius, Fikret Mamedov, Felix M. Ho,* and Stenbjörn Styring*

Molecular Biomimetics, Department of Photochemistry and Molecular Science, Ångström Laboratory, Uppsala University, SE-751 20 Uppsala, Sweden

Received February 17, 2006; Revised Manuscript Received April 7, 2006

ABSTRACT: Methanol binds to the $CaMn_4$ cluster in photosystem II (PSII). Here we report the methanol dependence of the split EPR signals originating from the magnetic interaction between the $CaMn_4$ cluster and the $Y_Z^•$ radical in PSII which are induced by illumination at 5 K. We found that the magnitudes of the "split S_1" and "split S_3" signals induced in the S_1 and S_3 states of PSII centers, respectively, are diminished with an increase in the methanol concentration. The methanol concentrations at which half of the respective spectral changes had occurred ($[MeOH]_{1/2}$) were 0.12 and 0.57%, respectively. By contrast, the "split S_0" signal induced in the S_0 state is broadened, and its amplitude is enhanced. $[MeOH]_{1/2}$ for this change was found to be 0.54%. We discuss these observations with respect to the location and nature of the methanol binding site. Furthermore, by comparing this behavior with methanol effects reported for other EPR signals in the different S states, we propose that the observed methanol-dependent changes in the split S_1 and split S_0 EPR signals are caused by an increase in the extent of magnetic coupling within the cluster.

In oxygenic photosynthesis, light-driven water oxidation to molecular oxygen is carried out by the water-oxidizing complex (WOC)[1] in PSII. The catalytic center is a $CaMn_4$ cluster acting together with the nearby, redox-active tyrosine residue Y_Z. According to the available crystal structures (*1*−*4*), the shortest distance between Y_Z and the $CaMn_4$ cluster is 5.4 Å. During water oxidation, the $CaMn_4$ complex cycles through five intermediate oxidation states in the so-called S state cycle [also termed the Kok cycle (*5*)]. Using well-developed experimental protocols, the different S states, denoted S_n ($n = 0-4$), can be trapped by exposing PSII samples to varying numbers of saturating laser flashes followed by rapid freezing (see below). EPR spectroscopy is a powerful technique for characterizing the S states, and information-rich EPR spectra have been reported from the WOC in all S states except the transient S_4 state (for reviews, see refs *6*−*9*).

When intact PSII, trapped in different S states, is exposed to weak visible light at liquid helium temperatures, a series of EPR signals centered around $g \sim 2.0$ are induced in the S_1, S_3, and S_0 states (*10*−*18*). [In the S_1 and S_3 states, the signals can also be induced by NIR light (*13*, *19*−*21*).] These EPR signals are assigned as split radical EPR signals and are generally considered to originate from magnetic interactions between $Y_Z^•$ and the $CaMn_4$ cluster. In this paper, they are termed the "split S_1", "split S_3", and "split S_0" signals, according to the respective S state of the $CaMn_4$ cluster when the signals are induced. Figure 1 shows the spectra of these EPR split signals originating from PSII samples given different numbers of laser flashes. The formation and interpretations of these EPR split signals have been discussed in detail by several groups (*10*−*16*).

Many studies have indicated that the magnetic properties of the $CaMn_4$ cluster are modified by the presence or absence of methanol in an S state-dependent manner (*19*, *21*−*29*; Table 1). Since the S state-dependent split EPR signals originate from magnetic interactions between the $CaMn_4$ cluster and $Y_Z^•$, they might also be influenced by methanol. In this study, we describe how methanol affects these split EPR signals in the S_0, S_1, and S_3 states and determine the concentration dependence of the spectrally distinguishable changes. These data are compared with the effect of methanol on other EPR signals from the WOC and are discussed in an effort to improve our understanding of the magnetic properties of the $CaMn_4$ cluster and its magnetic interaction with the nearby $Y_Z^•$.

† The financial support from the Swedish Research Council, the European Community Sixth Framework Programme Marie Curie Incoming International Fellowship (514817 to F.M.H.), the Swedish Energy Agency, and the Knut and Alice Wallenberg Foundation is gratefully acknowledged.

* To whom correspondence should be addressed. Telephone: +46 18 471 6580. Fax: +46 18 55 9885. E-mail: felix.ho@fotomol.uu.se and stenbjorn.styring@fotomol.uu.se.

‡ Current address: Max Planck Institute for Bioinorganic Chemistry, Stiftstrasse 34−36, D-45470 Mülheim an der Ruhr, Germany.

[1] Abbreviations: Chl, chlorophyll; DAD, 3,6-diaminodurol; DMSO, dimethyl sulfoxide; EPR, electron paramagnetic resonance; EXAFS, extended X-ray absorption fine structure; MES, 2-(*N*-morpholino)-ethanesulfonic acid; MeOH, methanol; $[MeOH]_{1/2}$, methanol concentration at which half of the change in the corresponding EPR spectrum has occurred; NIR, near-infrared; P_{680}, primary electron donor in PSII; PpBQ, phenyl-*p*-benzoquinone; PSII, photosystem II; XANES, X-ray absorption near-edge spectroscopy; Y_D, redox-active Tyr_{161} in the D2 protein of PSII; Y_Z, redox-active Tyr_{160} in the D1 protein of PSII; WOC, water-oxidizing complex; Car, carotenoid; Cyt, cytochrome.

10.1021/bi060333u CCC: $33.50
Published on Web 05/26/2006

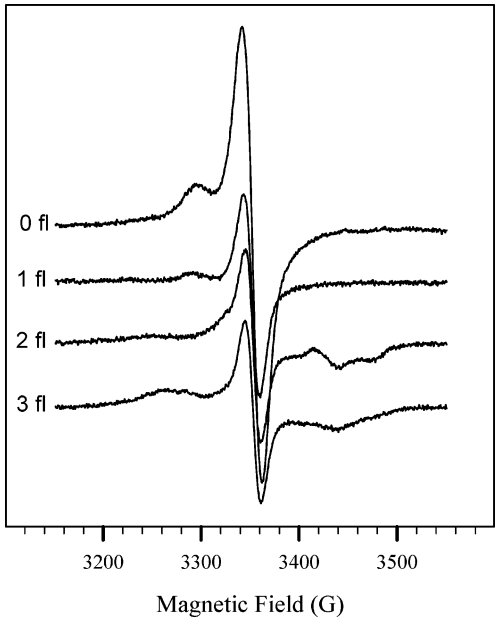

FIGURE 1: EPR spectra recorded in pre-reduced PSII given zero to three laser flashes. The spectra are the light-minus-dark difference spectra between spectra recorded immediately after illumination for 20 s at 5 K and spectra recorded before illumination. The figures indicate the number of flashes given. The applied light intensity was 80 W/m^2. EPR conditions: microwave power of 25 mW, microwave frequency of 9.47 GHz, modulation amplitude of 10 G, and temperature of 5 K.

Table 1: Methanol Dependence of EPR Signals in PSII

S state	EPR signal	MeOH effect	MeOH $[MeOH]_{1/2}$	refs
S_0	S_0 multiline	appears	0.40%	*33*
	split S_0 signal	modifies signal shape	0.54%[a]	this study
S_1	S_1 $g \sim 4.9$[b]	disappears	nr[c]	*28*
	split S_1 signal	disappears	0.12%[a]	this study
S_2	S_2 multiline	amplitude increases	0.35%	*33*
	S_2 $g \sim 4.1$	disappears	0.20%	*33*
S_3	S_3 $g \sim 8$ and 12[b]	disappears	nr[c]	*19, 29*
	split S_3 signal	disappears	0.57%[a]	this study

[a] The estimated experimental error in $[MeOH]_{1/2}$ is ±0.05%. [b] Changes observed in EPR signals detected with parallel-mode EPR. [c] Not reported.

MATERIALS AND METHODS

PSII-enriched membranes (BBY) were prepared from hydroponically grown greenhouse spinach as described by Berthold et al. (*30*), with modifications according to Völker et al. (*31*), suspended in a buffer containing 0.4 M sucrose, 25 mM MES-NaOH (pH 6.1), 15 mM NaCl, and 3 mM $MgCl_2$, and then stored at −80 °C before being used. The Chl concentration was determined according to the method of Arnon (*32*). The rate of oxygen evolution, measured with a Clarke oxygen electrode (Hansatech) in the presence of 1.0 mM PPBQ as an electron acceptor, was 400−450 μmol of O_2 (mg of Chl)$^{-1}$ h^{-1}. The presence of methanol up to 5% (v/v) did not effect oxygen evolution (see also ref *33*).

Chemical reduction of $Y_D^\bullet$ to 5−10% of its maximum size was accomplished by reduction with ascorbate (10 mM) and DAD (3 mM) for 30 min and subsequent removal of the reagents by washing and centrifugation as described by Feyziyev et al. (*34*) to prevent the large signal from $Y_D^\bullet$ in the $g \sim 2$ region of the EPR spectrum. The chemical reduction procedure was completed within 1−2 h. All steps after the addition of ascorbate and DAD were performed in complete darkness to prevent reoxidation of Y_D.

After the reduction of $Y_D^\bullet$, PpBQ was added as an external electron acceptor (from a 50 mM stock solution in DMSO) and the samples were transferred to calibrated EPR tubes. Where used, the required amount of methanol was first added to the empty EPR tubes before the treated BBY samples were added and mixed. The final concentrations of Chl, PpBQ, and DMSO were 2.7−3.3 mg/mL, 1 mM, and 1% (v/v), respectively.

After the samples had been equilibrated to 0 °C by immersion in an ethanol/ice bath, they were illuminated with zero, one, two, and three laser flashes from a Nd:YAG laser (6 ns, 532 nm, 440 mJ/pulse) to predominantly induce the S_1−S_3 and S_0 states, respectively. After flashing had been carried out, the samples were frozen within 1−2 s in an ethanol/solid CO_2 bath and then rapidly transferred to liquid nitrogen.

Induction of the split signals by white light illumination at 5 K was carried out directly into the Bruker ST4102 standard EPR cavity as in Zhang and Styring (*14*). The light was provided by a 150 W projector using a Perspex light guide. A neutral density filter (Schott NG9) was used to obtain the appropriate light intensity, and a 5 cm thick $CuSO_4$/water solution was used to cut off the longer wavelengths (>700 nm). The final light intensity provided in a particular experiment was measured at the position of the EPR cavity with a light meter (Li-Cor Inc., LI-1858, fitted with a LI-190SB quantum sensor). Low-temperature EPR spectra were recorded on a Bruker ELEXYS E500 spectrometer equipped with an Oxford-900 liquid helium cryostat and an ITC-503 temperature controller (Oxford Instruments Ltd.). The other experimental settings are given in the figure legends. All data acquisition was carried out by the Bruker Xepr software. Most of the presented spectra are difference spectra where the spectrum recorded prior to low-temperature illumination has been subtracted from the spectrum recorded immediately after (or sometimes during) the illumination.

RESULTS

Induction of Split EPR Signals in Different S States by Illumination at 5 K. The induction of the split EPR signals in PSII samples poised in different S states was achieved by 20 s illumination at 5 K directly into the EPR spectrometer. Figure 1 shows the light-minus-dark difference spectra, obtained in the absence of methanol, in samples provided with zero to three laser flashes to turn the PSII $CaMn_4$ cluster over to different S states. In the dark-adapted sample (Figure 1, zero flashes), the split S_1 signal was formed, reflecting that the S_1 state dominated in this sample. This signal is characterized by a low-field peak centered at 3290 G, which, due to misses in the flash transition, was also visible to a small extent in the sample provided with one flash, similar to what has been described previously (*14*, *18*). The sample provided with two flashes was dominated by a different split S_3 signal, which showed a wide high-field trough with a minimum at 3440 G together with a weak peak at 3250 G. It is noteworthy that the split S_3 signal induced by visible illumination as described here is the same signal that was obtained by illumination with NIR light (*19*−*21*).[2] In the

latter case, the induction of the signal was assigned to absorption by the $CaMn_4$ cluster in the S_3 state (*19*−*21*). In the sample exposed to three flashes, the spectrum from the split S_0 signal was induced. This signal is more symmetric, with a significant low-field peak at 3270 G and a high-field trough at 3435 G, similar to the signal reported earlier by Zhang and Styring (*14*) and Zhang et al. (*16*). It should be noted that the sample after three flashes still contained a significant contribution from the S_3 state, reflecting dephasing of the S cycle due to misses (*5*, *35*, *36*). Consequently, the spectrum recorded after three flashes contained a mixture of split S_0 and split S_3 signals (see below).

In addition to these spectral features, which have been described before, all three split signals exhibited a central, symmetrical feature at $g \sim 2$. This feature can be observed in our spectra since Y_D was reduced. [Note that for S state turnovers, laser flashes were applied to the samples at 0 °C. Y_D reoxidation is slow at our time scales under these conditions (*34*). EPR spectra revealed that our flash protocol led to no oxidation of Y_D (not shown), and thus, $Y_D^{\bullet}$ did not contribute to the difference spectra.] This central feature has also been described in a mutant lacking Y_D (*37*). We have previously reported preliminary studies of the decay-associated spectra and the microwave relaxation properties of all spectral parts of these three split signals, including this middle part (*17*). Here, we investigate the effect of methanol at different concentrations on each of the three split signals.

Effect of Methanol on the Split S_1 Signal. Figure 2A shows the split S_1 signal induced in dark-adapted samples in the presence of different concentrations of methanol. As the methanol concentration increased, the split signal intensity decreased, both at the low-field peak centered at 3290 G and in the central region of the signal. The split signal amplitude (measured at the peak at 3290 G, Figure 2B) was very sensitive to the presence of methanol and was close to zero at a concentration of 1%. $[MeOH]_{1/2}$ for the decrease in the signal amplitude was found to be 0.12% (30 mM, Table 1). The concentration dependence of the amplitude decrease was found to be uniform across the entire signal (not shown).

At >3% methanol, there was no signal amplitude remaining at the low-field peak, but there still remained a fraction of the radical-like feature located in the $g \sim 2$ region of the spectrum. This feature was already observable at a methanol concentration of 1% (Figure 2A) and was insensitive to increasing methanol concentration (not shown). We suggest that the methanol-insensitive spectrum represents another light-induced species that was also formed with our illumination at 5 K, irrespective of the presence or absence of methanol. This species is most likely an oxidized chlorophyll and/or carotenoid radical in the Car−Chl_Z−Cyt b_{559} pathway known to be functional at these very low temperatures (*38*−*42*). Formation of the split signal together with a Chl/Car radical species has been observed previously (*14*, *16*).

The inset in Figure 2B shows a double difference spectrum that was obtained by subtraction of the light-minus-dark spectrum of the 3% methanol sample (representing the light-induced signal in the presence of methanol, i.e., a spectrum lacking the split S_1 signal) from the corresponding spectrum from the sample containing no methanol (representing the light-induced signals including the split S_1 signal). Since the induction of the putative chlorophyll/carotenoid radical can be expected to be the same irrespective of the methanol concentration, this radical will not contaminate the resulting spectrum. We conclude therefore that this double difference spectrum is the purest split S_1 signal we can obtain under our experimental conditions.

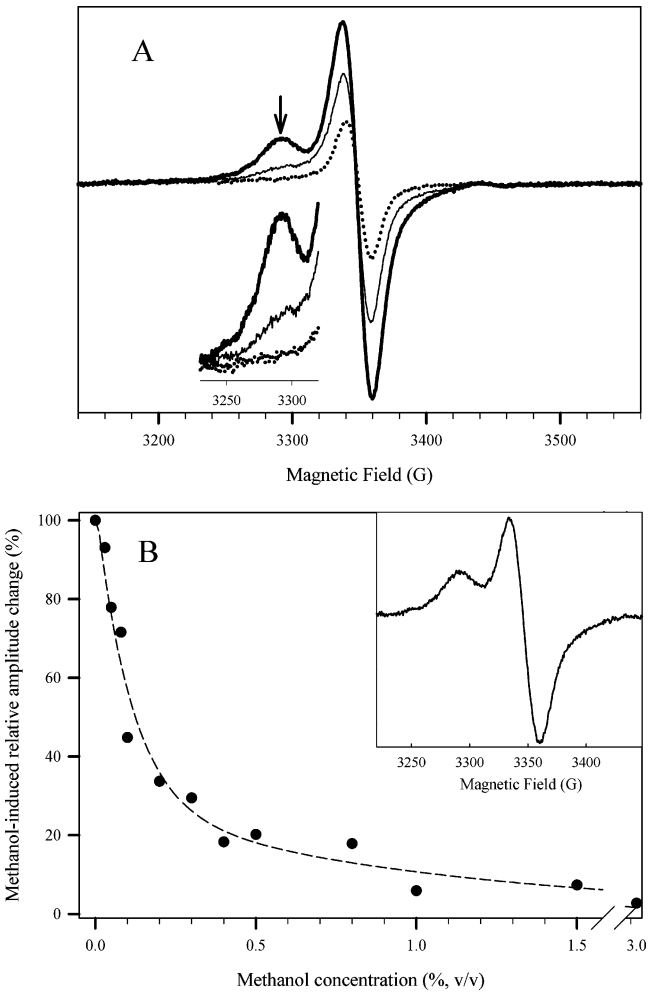

FIGURE 2: Methanol concentration dependence of the split S_1 EPR signal from dark-adapted samples illuminated at 5 K. (A) Light-minus-dark difference spectra (including the inset, which shows the amplification of the signal peak centered at 3290 G) obtained at 0% (thick line), 0.2% (thin line), and 1.0% (dotted line) methanol. (B) Normalized amplitude at 3290 G (marked with an arrow in panel A) showing the methanol dependence of the signal amplitude. The inset shows the double difference spectrum obtained by subtracting the light-minus-dark spectrum of the sample containing 3% methanol from the light-minus-dark spectrum of the sample containing no methanol. EPR and illumination conditions were as described in the legend of Figure 1.

Effect of Methanol on the Split S_3 Signal. The dependence of the split S_3 signal on the methanol concentration is shown in Figure 3A. The application of two laser flashes to the PSII sample in the presence of pre-reduced Y_D resulted in a sample dominated by the S_3 state, but with some PSII centers remaining in the S_2 state due to misses in the flash-induced transition of the $CaMn_4$ cluster. However, the S_2 state does not give rise to a split signal induced by illumination at 5 K

[2] A full investigation of the wavelength-dependent induction of these S state-dependent split EPR signals using monochromatic laser light between 420 and 900 nm is in progress.

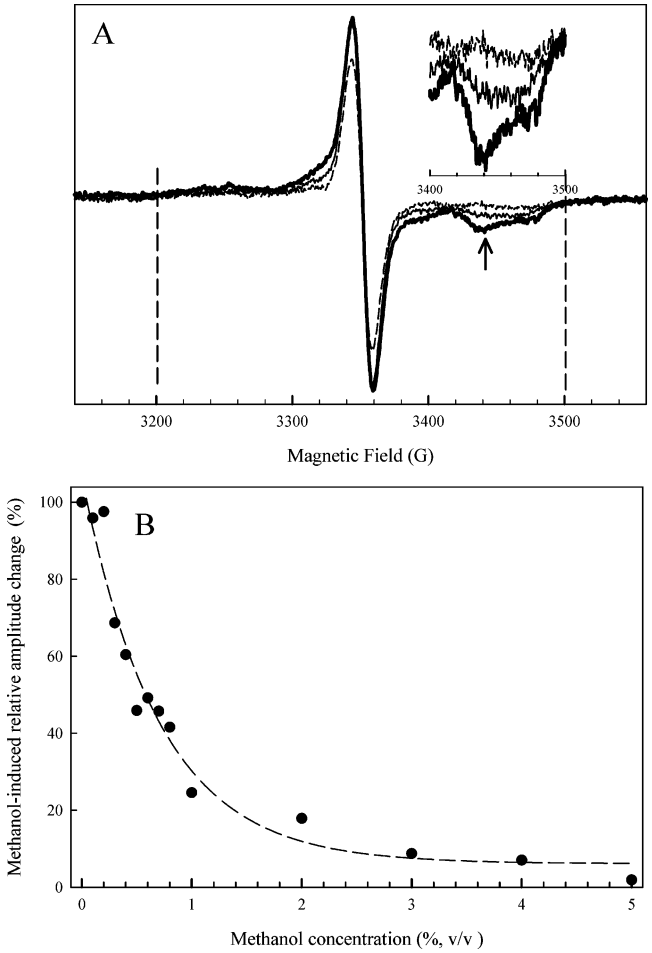

FIGURE 3: Methanol concentration dependence of the split S_3 EPR signal induced by illumination at 5 K of samples exposed to two flashes. (A) Light-minus-dark difference spectra (including the inset, which shows the amplification of the signal trough centered at 3440 G) obtained at 0% (thick line), 0.5% (thin line), and 3.0% (dotted line) methanol. The dashed lines indicate the field positions used for comparison with the split S_0 signal (see Figure 4 and accompanying text for details). (B) Normalized amplitude change at 3440 G (marked with an arrow in panel A) showing the methanol dependence of the signal amplitude. EPR and illumination conditions were as described in the legend of Figure 1.

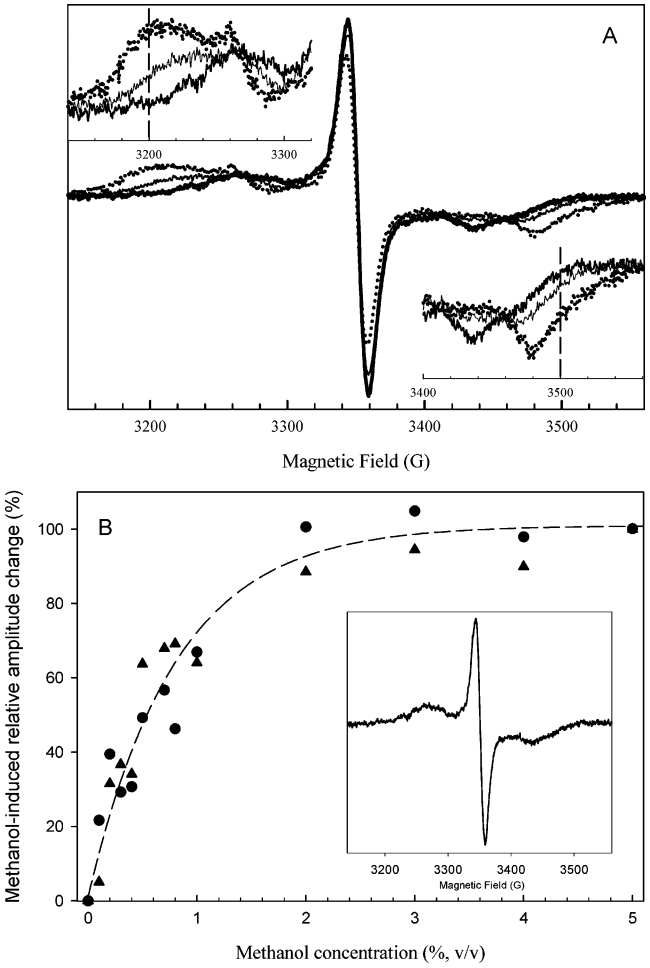

FIGURE 4: Methanol concentration dependence of the split S_0 EPR signal induced by illumination at 5 K of samples exposed to three flashes. (A) Light-minus-dark difference spectra (including the insets, which show the amplification of the signals in the main spectra) obtained at 0% (thick line), 0.5% (thin line), and 3.0% (dotted line) methanol. The dashed lines indicate the position used for plotting panel B. (B) Normalized amplitude change at 3200 (▲) and 3500 G (●) showing the methanol dependence of the appearance of the methanol form of the split S_0 signal. The inset shows the corrected split S_0 signal in the absence of methanol. Contributions from the split S_3 signal were removed by subtraction (see text for details). EPR and illumination conditions were as described in the legend of Figure 1.

in intact PSII samples (*10*, *14*). Therefore, there was no contribution from S_2 centers to the light-induced split EPR signal in the two-flash sample. Instead, the observed EPR signal reflects only PSII centers that were in the S_3 state after the two flashes.

The spectra in Figure 3A clearly show that the amplitude of the split S_3 signal decreases in the presence of methanol. This was best observed on the high-field side of $g = 2$ (Figure 3A, inset). The signal was large in the absence of methanol, much smaller at 0.5% methanol, and almost absent in the presence of 3% methanol. The methanol concentration dependence of the decrease in the split S_3 signal, monitored at the high-field trough at 3440 G (an arrow in Figure 3A), is shown in Figure 3B. $[MeOH]_{1/2}$ for the signal decrease was estimated to be 0.57% (140 mM, Table 1). The concentration dependence of the amplitude change was uniform across the entire signal (not shown).

Effect of Methanol on the Split S_0 Signal. Figure 4A shows the methanol concentration dependence of the light-minus-dark difference spectra of samples given three flashes, recorded after illumination at 5 K. In these spectra, the analysis was more complex than for the split S_1 or split S_3 signals. There were two reasons for this. First, as in the case of the S_3 state, the transition in the three flashes to the S_0 state entails significant S state mixing, and a significant number of S_3 centers remain in the sample. This complicates the analysis, since the S_3 state also gives rise to its own split signal with its own methanol dependence. Second, the spectra in Figure 4A immediately reveal that the split S_0 signal did not disappear (as was the case for the split S_3 signal) as the methanol concentration increased. Instead, the spectral shape was altered.

The methanol concentration dependence of the spectral changes in the split S_0 signal is depicted in Figure 4B. Here we have plotted the amplitude changes at 3200 and 3500 G (dashed lines in Figure 4A). At these field positions, neither the split S_3 signal (compare dashed lines in Figure 3) nor the split S_0 signal in the absence of methanol had any signal

amplitude. Thus, the amplitude changes only reflected the appearance of the new methanol form of the split S_0 signal. Maximum intensities were reached at ~3% methanol for both field positions. The methanol dependence for the formation of both peaks was very similar, which strongly suggests that they are directly linked to one another. Taking these two methanol dependences to be the same, we determined the $[MeOH]_{1/2}$ to be 0.54% (135 mM, Table 1).

To analyze these complex spectral changes in detail, we attempted to isolate the contribution from the methanol-induced changes in the split S_0 signal from methanol-induced changes in the split S_3 signal by subtraction of the S_3 part of the spectra in Figure 4. This proved difficult mainly because the split S_3 signal was also altered by methanol (Figure 3). However, to allow comparison between the two forms of the split S_0 signal, a weighted fraction of the split S_3 signal in the absence of methanol, corresponding to 35% of the PSII centers, was subtracted from the spectrum of the 0% methanol sample in Figure 4A. The resulting spectrum is shown in the inset of Figure 4B. The estimation that ca. 35% of the PSII centers remain in the S_3 state after three flashes is reasonable in our type of samples with reduced Y_D, where a synchronizing preflash (*25*, *43*) could not be used.

It is interesting to compare the split S_0 signals in the presence and absence of methanol. In the absence of methanol, the split S_0 signal was similar to those observed earlier (*14*, *16*). In the presence of methanol, the spectral modification is very clear at the low-field side of $g = 2$. Whereas the spectrum in the absence of methanol was dominated by the peak at 3270 G, with virtually no amplitude below 3220 G, in the presence of methanol, a large peak centered around 3210 G, with an overlapping peak at 3260 G, appeared in a methanol-dependent manner. There still remained signal amplitude at 3270 G in the presence of methanol, but careful inspection of the spectrum reveals that the earlier peak was now absent (this is clearly seen at 3290 G where no amplitude remained at 5% methanol). Instead, the remaining amplitude at 3270 G reflects the fact that the new peaks observed upon methanol addition also have amplitude here. Thus, it seems that the split S_0 signal did not disappear in the presence of methanol but rather that methanol induced large modifications in the shape of the EPR spectrum.

The altered spectral shape in the presence of methanol was also observable at the high-field side of $g = 2$. Here the signal was dominated by a peak centered at 3435 G in the absence of methanol. With the addition of methanol, the shape changed and the spectrum became dominated by a sharp trough around 3480 G, where there was virtually no amplitude in the absence of methanol.

Effect of S_0 Split Signal Induction on the S_0 Multiline Signal. The S_0 state gives rise to a multiline signal in the presence of methanol (*25*−*27*, *33*, *44*−*47*). Thus, it was interesting to investigate if the induction of the split S_0 signal by illumination at 5 K had any effect on the S_0 multiline signal. This was tested in a sample given three flashes. Due to misses in the S state transitions, the sample contained a mixture of S_0-, S_3-, and S_2 state centers. Therefore, to facilitate analysis, the contribution to the EPR spectra from the S_2 multiline signal from the S_2 centers was removed by weighted subtraction (not shown) using procedures described previously (*25*, *48*). The resulting spectra are shown in Figure 5.

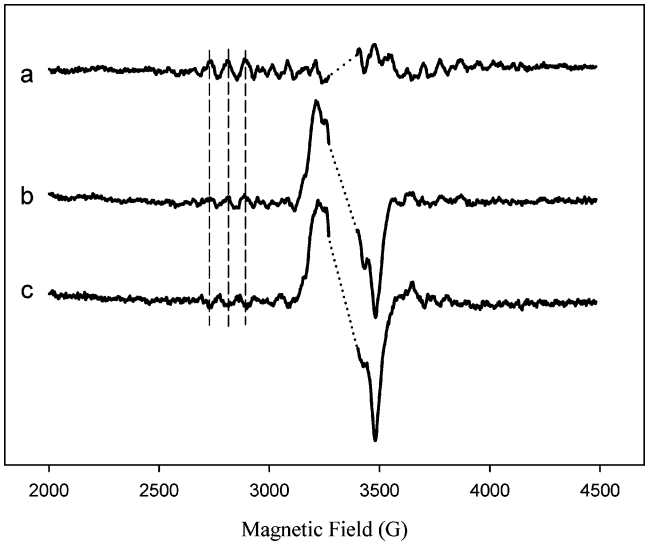

FIGURE 5: Light-induced changes in the S_0 multiline and split S_0 signals recorded in the same sample. (a) S_0 multiline signal of a three-flash sample containing 5% (v/v) methanol, measured in the dark at 5 K. (b) The same three-flash sample measured during continuous illumination (80 W/m^2) at 5 K to induce a steady-state split S_0 signal. (c) Light-minus-dark difference spectrum obtained by subtracting spectrum a from spectrum b. EPR conditions: microwave power of 25 mW, microwave frequency of 9.47 GHz, modulation amplitude of 15 G, scan time of 168 s, conversion time of 82 ms, four scans, and temperature of 5 K. Residual S_2 multiline signals in the spectra were subtracted as described in the text.

In the dark (Figure 5, spectrum a), the S_0 multiline signal was observed (typical peaks indicated with dashed lines). The split S_0 signal was then induced by illumination at 5 K. Since the split S_0 signal decays quite rapidly in the dark ($t_{1/2} \sim 3-5$ min; *14*, *16*, *17*), the sample in this particular experiment was illuminated during the entire EPR scan, in total for 11 min (Figure 5, spectrum b). The illumination resulted in a large increase in the intensity around $g = 2$, reflecting the formation of the methanol form of the split S_0 signal (cf. Figure 4), as well as subtle changes in peaks of the S_0 multiline EPR signal farther from the center.

Already from spectrum b, it was clear that the illumination at 5 K resulted in the formation of the split S_0 signal concomitantly with changes in the S_0 multiline signal peaks. These changes are better displayed in the light-minus-dark difference spectrum c (Figure 5). The split signal is clearly visible, with the characteristic peaks at 3210 and 3480 G dominating the spectrum. However, the changes in the multiline peaks now became clearly observable and possible to analyze. Close examination of the changes revealed that they occurred exactly at the field positions for peaks originating from the S_0 multiline signal (dashed lines in Figure 5). However, they were inverted. Consequently, they represented a decrease in the amplitude of the S_0 multiline signal, induced by illumination at 5 K and occurring simultaneously with the formation of the split S_0 signal. The decrease in the S_0 multiline signal represented ca. 40% of the signal amplitude, which is similar to literature estimates of the centers in the S_0 state that gave rise to the split S_0 signal [in 40−50% of the S_0 centers (*14*, *16*)].

Table 2: Effect of Methanol on the Energy Gap between the Ground and First-Excited Spin States of the $CaMn_4$ Complex in the Different S States

S state (EPR signal)	Δ (cm^{-1})[a] without MeOH	with MeOH	refs[b]
S_0 (multiline)	na[f]	31,[c] 22[d]	*79*, *47*
S_1 (parallel mode $g \sim 4.9$)	1.7[e]	10[e]	*28*
S_2 (multiline)	na,[f] 6[c]	12,[c] 30[d]	*79*, *76*
S_3 (parallel mode $g \sim 8$ and 12)	2.4[e]	na[f]	*29*

[a] Energy gap between the ground and first-excited spin states of the $CaMn_4$ cluster. [b] Where more than one source is used, the references are shown in the order of the cited values. [c] Assuming $\Delta = |3J|$. [d] Obtained from an Orbach plot. [e] Assuming $\Delta = |2J|$. [f] Not available.

DISCUSSION

EPR Signal Alternations Due to Methanol. Many effector molecules [for example, Ca^{2+} and NH_3 (*49*−*55*)] bind to and affect the $CaMn_4$ cluster in an S state-dependent manner. This also holds for methanol, and work by many laboratories has revealed that methanol modifies EPR signals from the WOC in all S states. Table 1 provides a compilation of the main methanol effects on the S state-dependent EPR signals. One prominent effect of binding of methanol to the WOC is that the S_0 state gives rise to a multiline EPR signal in plants only in the presence of methanol (*25*−*27*, *33*, *44*−*47*). A similar effect holds for the S_2 state multiline signal, which increases in intensity and undergoes a change in spectral appearance in the presence of methanol (*23*, *33*, *56*). By contrast, methanol has been found to abolish other Mn-derived EPR signals from the S_1 state (the parallel mode $g = 4.9$ signal), the S_2 state (the $g = 4.1$ signal), and the S_3 state (the parallel mode $g = 8$ and 12 signals) (*19*, *28*, *29*, *33*). All these Mn-derived EPR signals reflect complex magnetic interactions between the Mn ions in the $CaMn_4$ complex, and it is thought that binding of methanol to the WOC changes the magnetic couplings between the Mn ions, thereby changing the EPR signals (Table 2; further discussions below). For the S_2 multiline signal, the exchange coupling parameter has been experimentally determined both in the presence and in the absence of methanol, while this does not hold for the other signals, which either appear or disappear in the presence of methanol.

All these observations reveal that methanol interacts closely with the $CaMn_4$ cluster in all S states. Two important questions are (i) where the site for methanol binding is and whether this site changes with S state and (ii) by which physicochemical mechanism methanol can define the increase or decrease in the magnitude of the EPR signals from the $CaMn_4$ cluster that reflect different, S state-dependent, magnetic properties in the Mn ensemble. We address both issues in the discussion of our results.

Binding of Methanol to the $CaMn_4$ Cluster. Little is known about the binding site for methanol in S states other than S_2 (see below). It is, however, likely that conclusions can be drawn from the concentration dependence for methanol-induced effects on a particular EPR signal (Table 1). This was used in an earlier study from our laboratory (*33*; reviewed in ref *45*) where it was found that the concentration dependences for the binding of methanol to the S_2 and S_0 states were quite similar [though not identical, and dependent on other additives (*33*); see also Table 1]. It was concluded that the methanol binding site was probably the same in both S states. In this paper, we have taken this study further to study the low-temperature-induced split EPR signals from the WOC. This allows us to draw conclusions about methanol binding in all S states.

In the S_0 state, we have now studied two spectral probes that are sensitive to the presence of methanol. The S_0 multiline signal appears in the presence of methanol, while the spectral shape of the split S_0 signal is altered in a significant manner. $[MeOH]_{1/2}$ for the appearance of the S_0 multiline signal is 0.40% (*33*) and for the spectral change in the split S_0 signal 0.54% (Table 1). These values are quite similar, and we conclude that both spectral modifications most likely involve the binding of methanol to the same site in the environment of Y_Z and the $CaMn_4$ cluster. Whether more than one methanol molecule is involved cannot be addressed quantitatively from the data presented here.

Binding of methanol to the WOC in the S_1 and S_3 states has not been carefully investigated, but it is known that the small and difficult to study Mn-dependent EPR signals, which can be observed in parallel mode EPR at high g values, are all abolished by the presence of methanol (Table 1 and the references cited). We have now determined $[MeOH]_{1/2}$ for modifications of both split S_1 and split S_3 signals, thereby providing binding data also in these S states (Table 1). $[MeOH]_{1/2}$ in the S_3 state is 0.57%, whereas methanol binding is more efficient in inhibiting formation of the split S_1 signal with a $[MeOH]_{1/2}$ 0.12%.

With $[MeOH]_{1/2}$ values now available for each of the S states (Table 1), it can be seen that the values fall into two groups. $[MeOH]_{1/2}$ values for the S_1 and S_2 states are similar to each other (average of 0.22%, range of $\pm$0.13%) and are significantly lower than in the S_3 and S_0 states. The $[MeOH]_{1/2}$ values of the S_3 and S_0 states are again similar to each other (average of 0.50%, range of $\pm$0.10%).

Detailed structural investigations of methanol binding have so far been restricted to the S_2 state. Force et al. (*22*) investigated interactions of methanol with the $CaMn_4$ cluster in the S_2 state using deuterium-labeled methanol (CD_3OD). Simulation of their three-pulse ESEEM time domain data indicated that the distance between the methanol protons and the Mn ions was 2.9−4.1 Å, close enough for methanol to be a direct ligand. More recently, Åhrling et al. (*23*) also concluded that methanol binds to Mn. Analysis of ESEEM spectra from the S_2 multiline signal led the authors to the conclusion that methanol most likely binds to a five-coordinate Mn^{III} ion in the cluster. This is one of the few pieces of experimental evidence of the presence of five-coordinate Mn^{III} in the S_2 state. It is interesting that further support for the existence of such a five-coordinate Mn^{III} in the S_2 state can be found in the recent time-resolved X-ray studies by Haumann et al. (*57*).

There is less knowledge about the methanol binding site in the other S states. However, from our binding data and information in the literature, some conclusions can be drawn. $[MeOH]_{1/2}$ in the S_1 state is similar to $[MeOH]_{1/2}$ in the S_2 state (Table 1), and we interpret this as a reflection of binding of methanol to a site with similar environments in both S states. This is substantiated by the consensus that has been reached from EXAFS studies that reveal no structural changes in the $CaMn_4$ cluster in the $S_1 \rightarrow S_2$ transition despite oxidation of one of the Mn ions (*57*−*62*).

The situation is different in the S_0 and S_3 states, and EXAFS studies show that conformational changes involving the Mn ions occur in the $S_0 \rightarrow S_1$ and $S_2 \rightarrow S_3$ transitions (*57*, *59*, *60*, *63*, *64*). This is consistent with our $[MeOH]_{1/2}$ data in both the S_0 and S_3 states, which are different from $[MeOH]_{1/2}$ values in the S_1 and S_2 states (Table 1). However, in neither case is methanol likely to be completely without access to the Mn ion(s) since the presence of methanol perturbs all known EPR signals (Table 1). Therefore, in the absence of direct data for or against, we propose that methanol binding occurs in a coordination site of a Mn ion. Furthermore, the protein environment around the $CaMn_4$ cluster is densely packed, and the metal cluster is embedded deep in the large PSII protein. Therefore, methanol (and substrate water) access must be limited to defined channels extending through the protein. Possible channels for water and/or proton entry and exit have previously been proposed, on the basis of available crystal structures (*3*, *65*−*67*). Although EXAFS studies have revealed that the structure of the $CaMn_4$ cluster is altered during S state cycling, there is little reason to believe that the channels protruding far from the site are totally changed, making methanol access a different Mn ion several angstroms away. Instead, we propose that the methanol binding site remains at the same Mn ion in all S states. However, the structure of the $CaMn_4$ cluster remains the same only in the S_1 and S_2 states. Therefore, the conformations of the binding site on the Mn ion in the S_0 and S_3 states are different from the conformation in the S_1 and S_2 states, with the $CaMn_4$ cluster in the latter states showing greater sensitivity toward the presence of methanol. This is reflected in the lower $[MeOH]_{1/2}$ values for the S_1- and S_2 state signals.

Mechanism behind the Effects of Methanol on Split EPR Signals. The second issue we will discuss concerns the mechanism by which methanol can affect the low-temperature-induced split signals in the different S states. These signals reflect magnetic interaction of the $CaMn_4$ cluster in a particular S state with a nearby oxidized radical. This radical should be situated 6−10 Å from the interacting manganese ion(s) to give rise to these kind of split EPR signals (*68*−*74*). The radical is thought to be $Y_Z^{\bullet}$ formed by the illumination at 5 K. The main arguments behind this assignment are firstly the close position of Y_Z to the $CaMn_4$ cluster, and secondly by analogy to the split signals from $S_2Y_Z^{\bullet}$ observed in PSII inhibited by Ca^{2+} depletion or by the presence of acetate. Since methanol binds directly to Mn and also appears to alter the exchange couplings in the S state-dependent EPR signals from the $CaMn_4$ cluster (Table 2), it is likely that this is the cause of split signal modifications in the presence of methanol.

The starting point for our discussion of the effects of methanol on the split signals is the model of Koulougliotis et al. (*15*). According to this model, exchange interaction between the ground and first-excited states of the $CaMn_4$ cluster in the S_1 state ($S_a = 0$ and $S_a = 1$, respectively) with the organic radical (probably $Y_Z^{\bullet}$) gives rise to the spin multiplets M1 and M2, respectively (Figure 6A). The authors were able to successfully simulate the X- and W-band spectra of the split S_1 signal as originating from the M2 multiplet. Thus, both the S_1 state parallel mode EPR signal (*28*, *75*) and the split S_1 signal have been linked to the first-excited ($S = 1$) spin state of the $CaMn_4$ cluster.

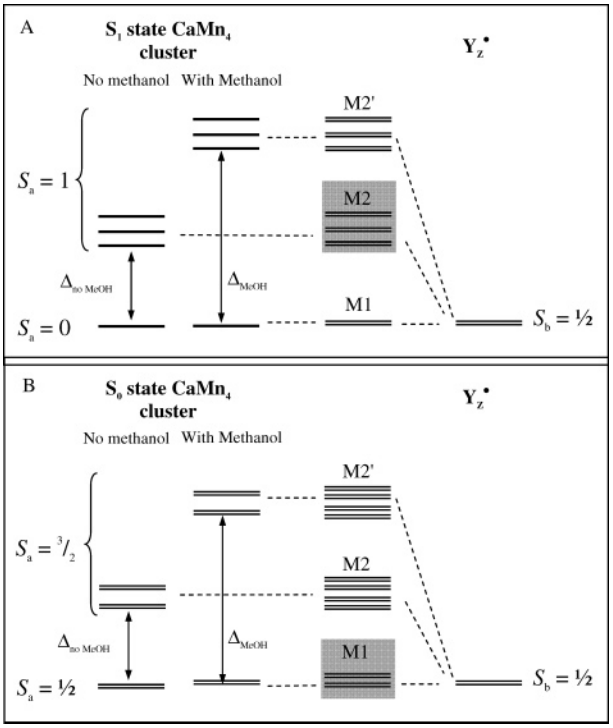

FIGURE 6: Schematic energy diagram of the spin states involved in the coupling of the $CaMn_4$ cluster in the (A) S_1 and (B) S_0 states with the $Y_Z^{\bullet}$ radical in the absence and presence of methanol. $\Delta_{no\ MeOH}$ and Δ_{MeOH} denote the energy gaps between the ground and first-excited spin states of the $CaMn_4$ cluster in the absence and presence of methanol, respectively (see Table 2 and accompanying text for the reported values of $\Delta_{no\ MeOH}$ and Δ_{MeOH}). Double lines represent Kramers doublets. The spin multiplet resulting from exchange interaction between $Y_Z^{\bullet}$ and the ground spin state of the $CaMn_4$ cluster is represented by M1, and the spin multiplets resulting from exchange interaction between $Y_Z^{\bullet}$ and the first-excited spin state of the $CaMn_4$ cluster in the absence and presence of methanol are represented by M2 and M2′, respectively. The spin multiplets assigned as the origins of the split S_1 and split S_0 signals are shaded.

Considering now the case in which methanol is present, the S_1 state parallel mode signal has been shown to be abolished by the presence of 3% methanol. The cause of this has been assigned to an increase in the Mn−Mn exchange coupling J value from $-0.87\ cm^{-1}$ to an estimated value of $5\ cm^{-1}$ (Table 2). The excited $S = 1$ state is thereby depopulated by moving it out of thermal reach (*28*). While this coupling value was calculated on the basis of a Mn dimer model so that $|2J| = \sim 10\ cm^{-1}$ may not be a true reflection of the actual energy gap between the $S = 0$ and $S = 1$ states (Δ_{MeOH} in Figure 6A) if all four Mn ions were to be magnetically coupled to each other (*46*), the effect of methanol increasing the gap is nevertheless reasonable. This increase in exchange coupling has also been observed for the S_2 multiline signal, where an increase from 6 to $30\ cm^{-1}$ in the presence of methanol has been reported (*76*). In other studies where calculations of the energy gap have yielded values of ∼30 (*77*) and $36.5 \pm 0.7\ cm^{-1}$ (*78*), ethanol was present in the sample buffer at a concentration of 4−5%.

We therefore postulate that the increase in Mn−Mn coupling due to the presence of methanol is the reason the split S_1 signal disappears. Since the split S_1 signal originates from the M2 multiplet (shaded area in Figure 6A), if the $S_a = 1$ state of the $CaMn_4$ cluster increases in energy and

becomes depopulated due to the presence of methanol (Δ_{MeOH} vs $\Delta_{no\ MeOH}$ in Figure 6A), the corresponding multiplet resulting from its interaction with $Y_Z^\bullet$ (labeled M2′ in Figure 6A) would also be depopulated (even assuming that the energy of the $S_a = 1$ state had not been increased to a level too high for interaction with the $S_b = {}^1/_2$ state of $Y_Z^\bullet$ to be possible). As the M2 multiplet is the attributed origin of the split S_1 signal, it is reasonable that the split signal should disappear upon methanol addition.

A similar kind of spin interaction analysis can be applied to the split S_0 signal (Figure 6B). Phenomenologically, the S_0 multiline signal is only observed in the presence of methanol, and in contrast to the S_1 state, illumination-induced split S_0 signals are observed both with and without methanol present, though with different spectral shapes (Figure 4).

We consider first the case in which methanol is present. Åhrling et al. (*79*) demonstrated that the S_0 multiline signal originates from an isolated $S = {}^1/_2$ ground state, with an energy gap between the ground and first-excited state (Δ_{MeOH} in Figure 6B) of 31 cm^{-1} as calculated from a dimer-of-dimers model. A recent calculation of this energy gap based on an Orbach plot of T_1 data gave a lower energy gap of 21.7 ± 0.4 cm^{-1} (*47*). In both cases, it was shown that the first-excited spin state is clearly out of thermal reach at 5 K ($kT = 3.5$ cm^{-1} at 5 K). Therefore, as in the previous analysis for the S_1 signals, the lack of population of the first-excited $S = {}^3/_2$ state implies that the M2 multiplet in the exchange-coupled system (Figure 6B) is also unpopulated. Hence, the fact that a split S_0 signal is observed despite the presence of methanol points to M1 as the origin of the split S_0 signal (shaded area in Figure 6B).

Our analysis indicates that, in the presence of methanol, it is the $S = {}^1/_2$ ground state of the $CaMn_4$ cluster that is involved in producing both the S_0 multiline signal and, when interacting with $Y_Z^\bullet$, the split S_0 signal. If correct, this model would predict that the centers where $Y_Z^\bullet$ is formed upon illumination at 5 K would no longer contribute to the S_0 multiline signal, as they now become exchange-coupled to the $CaMn_4$ cluster to give the M1 multiplet. A decrease in the S_0 multiline signal intensity would thus be expected as the split S_0 signal is induced. This prediction was borne out by the experiments described in Figure 5, where the S_0 multiline spectrum decreased in amplitude while the split S_0 signal was formed following illumination at 5 K. From this, we conclude that the split S_0 signal was formed at the expense of the S_0 multiline signal, supporting our analysis.

In accordance with our analysis, a smaller energy gap between the ground and first-excited spin states of the $CaMn_4$ cluster is expected in the absence of methanol ($\Delta_{no\ MeOH}$ in Figure 6B). The split S_0 signal is still observed, in agreement with the assignment of the origin of this signal to the lower-lying M1 multiplet (shaded area in Figure 6B), which would clearly remain populated. The different widths of the split S_0 signals with and without methanol (280 and 160 G, respectively; Figure 4) may reflect an increase in the level of interaction between $Y_Z^\bullet$ and the $CaMn_4$ cluster in the presence of methanol. In addition, the change in spectral shape upon methanol addition might reflect a change in the g and/or hyperfine anisotropy of the $CaMn_4$ cluster. Such changes have been shown to explain EPR spectral differences in the $S_2Y_Z^\bullet$ split EPR signals from acetate-treated and Ca^{2+}-depleted PSII (*74*).

A corollary of the hypothesis that the M1 multiplet is responsible for the split signals in the S_0 state is that, as the M2 multiplet increases in energy and becomes thermally inaccessible upon methanol addition (M2′ multiplet in Figure 6B), the population of M1 should increase. Therefore, the split signal should also become more intense. This is what was indeed observed: not only did the shape of the split S_0 signal change with an increase in methanol concentration, the peak area also increased. This was clearly visible in the spectra in Figure 4A. However, at present, it is not clear whether this intensity change also reflects altered magnetic properties of the species rather than purely an increased number of spins.

Our experiments do not address why an S_0 multiline is not observed without methanol addition, even though this signal originate from the $S = {}^1/_2$ state from which the M1 multiplet is derived. However, a broad, featureless ~2400 G wide S_0 signal has been reported in the absence of methanol (*26*). This broad signal was described to match the S_0 multiline signal in both g value and spectral breadth, and the authors proposed that the S_0 multiline signal (observed in the presence of methanol) was the same signal as the broad signal in the absence of methanol, but with altered hyperfine coupling between the Mn ions. Furthermore, an S_0 multiline signal can be observed in PSII isolated from *Thermosynechococcus elongatus*, even in the absence of methanol (*80*).

A detailed analysis of the methanol effects on the split S_3 signal, in the framework of magnetic interactions between the $CaMn_4$ cluster and $Y_Z^\bullet$, is not possible at present. Unlike the case for the split S_1 signal, there is no simulation available for the split S_3 signal. This is at least partly due to the problem that there is as yet no consensus about the redox state of the $CaMn_4$ cluster when the split S_3 signal is observed. It has been suggested that the split S_3 signal could involve an $S_2'Y_Z^\bullet$ species, where S_2' is a proton-deficient form of the S_2 state (*10*, *19*−*21*). This S_2' species is proposed to be formed by the $CaMn_4$ cluster in the S_3 state being excited by the NIR radiation used in those studies, thereby becoming able to oxidize the nearby Y_Z to $Y_Z^\bullet$ at 5 K. However, the proton lost during the catalytic $S_2 \rightarrow S_3$ transition is not replaced, leading to a proton-deficient state formally at the oxidation state of S_2. The spin state of such a proton-deficient state formed at 5 K is not known. Consequently, it would be premature to attempt our type of analysis for the split S_3 signal.

CONCLUSIONS

The concentration-dependent effects of methanol on the split EPR signals of the S_1, S_3, and S_0 states, induced by illumination at 5 K, have been investigated in this study, thereby giving a more complete picture of methanol effects for each of the S states. The methanol sensitivity of each state, measured in terms of $[MeOH]_{1/2}$, combined with current structural models of the $CaMn_4$ cluster, suggests that methanol binds to the same site in each of the S states, albeit with different conformations. In addition, the methanol-induced spectral modifications we observe in the split S_1 and split S_0 signals indicate that methanol binding affects the EPR signal via an increase of the energy gap between the ground state and the first-excited state of the $CaMn_4$ cluster.

Thus, methanol binding has a direct effect on the magnetic interactions within the cluster.

REFERENCES

1. Zouni, A., Witt, H. T., Kern, J., Fromme, P., Krauss, N., Saenger, W., and Orth, P. (2001) Crystal structure of photosystem II from *Synechococcus elongatus* at 3.8 Å resolution, *Nature 409*, 739−743.
2. Kamiya, N., and Shen, J. R. (2003) Crystal structure of oxygen-evolving photosystem II from *Thermosynechococcus vulcanus* at 3.7 Å resolution, *Proc. Natl. Acad. Sci. U.S.A. 100*, 98−103.
3. Ferreira, K. N., Iverson, T. M., Maghlaoui, K., Barber, J., and Iwata, S. (2004) Architecture of the photosynthetic oxygen-evolving center, *Science 303*, 1831−1838.
4. Loll, B., Kern, J., Saenger, W., Zouni, A., and Biesiadka, J. (2005) Towards complete cofactor arrangement in the 3.0 Å resolution structure of photosystem II, *Nature 438*, 1040−1044.
5. Kok, B., Forbush, B., and McGloin, M. (1970) Cooperation of charges in photosynthetic O_2 evolution. I. A linear four step mechanism, *Photochem. Photobiol. 11*, 457−475.
6. Miller, A.-F., and Brudvig, G. W. (1991) A guide to electron paramagnetic resonance spectroscopy of Photosystem II membranes, *Biochim. Biophys. Acta 1056*, 1−18.
7. Britt, R. D., Peloquin, J. M., and Campbell, K. A. (2000) Pulsed and parallel-polarization EPR characterization of the photosystem II oxygen-evolving complex, *Annu. Rev. Biophys. Biomol. Struct. 29*, 463−495.
8. Åhrling, K. A., and Styring, S. (2000) The manganese cluster in Photosystem II investigated by EPR spectroscopy, in *Probing photosynthesis: Mechanisms, regulation and adaptation* (Yunus, M., Pathre, U., and Mohanty, P., Eds.) pp 148−163, Taylor & Francis, London.
9. Peloquin, J. M., and Britt, R. D. (2001) EPR/ENDOR characterization of the physical and electronic structure of the OEC Mn cluster, *Biochim. Biophys. Acta 1503*, 96−111.
10. Petrouleas, V., Koulougliotis, D., and Ioannidis, N. (2005) Trapping of metalloradical intermediates of the S states at liquid helium temperatures. Overview of the phenomenology and mechanistic implications, *Biochemistry 44*, 6723−6728.
11. Nugent, J. H. A., Turconi, S., and Evans, M. C. W. (1997) EPR investigation of water oxidizing photosystem II: Detection of new EPR signals at cryogenic temperatures, *Biochemistry 36*, 7086−7096.
12. Nugent, J. H. A., Muhiuddin, I. P., and Evans, M. C. W. (2002) Electron transfer from the water oxidizing complex at cryogenic temperatures: The S_1 to S_2 step, *Biochemistry 41*, 4117−4126.
13. Koulougliotis, D., Shen, J. R., Ioannidis, N., and Petrouleas, V. (2003) Near-IR irradiation of the S_2 state of the water oxidizing complex of Photosystem II at liquid helium temperatures produces the metalloradical intermediate attributed to $S_1Y_Z^{\bullet}$, *Biochemistry 42*, 3045−3053.
14. Zhang, C., and Styring, S. (2003) Formation of split electron paramagnetic resonance signals in photosystem II suggests that tyrosine$_z$ can be photooxidized at 5 K in the S_0 and S_1 states of the oxygen-evolving complex, *Biochemistry 42*, 8066−8076.
15. Koulougliotis, D., Teutlolf, C., Sanakis, Y., Lubitz, W., and Petrouleas, V. (2004) $S_1Y_Z^{\bullet}$ metalloradical intermediate in photosystem II: An X- and W-band EPR study, *Phys. Chem. Chem. Phys. 6*, 4859−4863.
16. Zhang, C., Boussac, A., and Rutherford, A. W. (2004) Low-temperature electron transfer in photosystem II: A tyrosyl radical and semiquinone charge pair, *Biochemistry 43*, 13787−13795.
17. Sigfridsson, K. G. V., Su, J.-H., Feyziyev, Y., and Styring, S. (2005) The spectral resolution of the "Split S_1" and "Split S_0" EPR-signals from photosystem II induced by illumination at 5 K, in *Photosynthesis: Aspects to Global Perspectives* (van der Est, A., and Bruce, D., Eds.) pp 386−388, Alliance Communications Group, Lawrence, KS.
18. Su, J.-H., Sigfridsson, K. G. V., Feyziyev, Y., and Styring, S. (2005) Flash-number dependent oscillation of split EPR signals from OEC in PSII induced by illumination at 5 K, in *Photosynthesis: Aspects to Global Perspectives* (van der Est, A., and Bruce, D., Eds.) pp 404−406, Alliance Communications Group, Lawrence, KS.
19. Ioannidis, N., and Petrouleas, V. (2000) Electron paramagnetic resonance signals from the S_3 state of the oxygen-evolving complex. A broadened radical signal induced by low-temperature near-infrared light illumination, *Biochemistry 39*, 5246−5254.
20. Ioannidis, N., and Petrouleas, V. (2002) Decay products of the S_3 state of the oxygen-evolving complex of Photosystem II at cryogenic temperatures. Pathways to the formation of the $S = {}^7/_2$ S_2 state configuration, *Biochemistry 41*, 9580−9588.
21. Ioannidis, N., Nugent, J. H. A., and Petrouleas, V. (2002) Intermediates of the S_3 state of the oxygen-evolving complex of Photosystem II, *Biochemistry 41*, 9589−9600.
22. Force, D. A., Randall, D. W., Lorigan, G. A., Clemens, K. L., and Britt, R. D. (1998) ESEEM studies of alcohol binding to the manganese cluster of the oxygen evolving complex of Photosystem II, *J. Am. Chem. Soc. 120*, 13321−13333.
23. Åhrling, K. A., Evans, M. C. W., Nugent, J. H. A., and Pace, R. J. (2004) The two forms of the S_2 state multiline signal in Photosystem II: Effect of methanol and ethanol, *Biochim. Biophys. Acta 1656*, 66−77.
24. Zimmermann, J.-L., and Rutherford, A. W. (1986) Electron paramagnetic resonance properties of the S_2 state of the oxygen-evolving complex of Photosystem II, *Biochemistry 25*, 4609−4615.
25. Åhrling, K. A., Peterson, S., and Styring, S. (1997) An oscillating manganese electron paramagnetic resonance signal from the S_0 state of the oxygen evolving complex in photosystem II, *Biochemistry 36*, 13148−13152.
26. Messinger, J., Robblee, J. H., Yu, W. O., Sauer, K., Yachandra, V. K., and Klein, M. P. (1997) The S_0 state of the oxygen-evolving complex in photosystem II is paramagnetic: Detection of EPR multiline signal, *J. Am. Chem. Soc. 119*, 11349−11350.
27. Messinger, J., Nugent, J. H. A., and Evans, M. C. W. (1997) Detection of an EPR multiline signal for the S_0 state in photosystem II, *Biochemistry 36*, 11055−11060.
28. Yamauchi, T., Mino, H., Matsukawa, T., Kawamori, A., and Ono, T. (1997) Parallel polarization electron paramagnetic resonance studies of the S_1 state manganese cluster in the photosynthetic oxygen-evolving system, *Biochemistry 36*, 7520−7526.
29. Matsukawa, T., Mino, H., Yoneda, D., and Kawamori, A. (1999) Dual-mode EPR study of new signals from the S_3 state of oxygen-evolving complex in photosystem II, *Biochemistry 38*, 4072−4077.
30. Berthold, D. A., Babcock, G. T., and Yocum, C. F. (1981) A highly resolved, oxygen-evolving Photosystem II preparation from spinach thylakoid membranes: EPR and electron-transport properties**,** *FEBS Lett. 134*, 231−234.
31. Völker, M., Ono, T., Inoue, Y., and Renger, G. (1985) Effect of trypsin on PS-II particles. Correlation between Hill-activity, Mn-abundance and peptide pattern, *Biochim. Biophys. Acta 806*, 25−34.
32. Arnon, D. I. (1949) Copper enzymes in isolated chloroplasts. Polyphenoloxidase in *Beta vulgaris*, *Plant Physiol. 24*, 1−15.
33. Déak, Z., Peterson, S., Geijer, P., Åhrling, K. A., and Styring, S. (1999) Methanol modification of the electron paramagnetic resonance signals from the S_0 and S_2 states of the water-oxidizing complex of Photosystem II, *Biochim. Biophys. Acta 1412*, 240−249.
34. Feyziyev, Y., van Rotterdam, B. J., Bernat, G., and Styring, S. (2003) Electron transfer from cytochrome b_{559} and tyrosine$_D$ to the S_2 and S_3 states of the water oxidizing complex in photosystem II, *Chem. Phys. 294*, 415−431.
35. de Wijn, R., and van Gorkom, H. J. (2002) S State dependence of the miss probability in Photosystem II, *Photosynth. Res. 72*, 217−222.
36. Shinkarev, V. P. (2005) Flash-induced oxygen evolution in photosynthesis: Simple solution for the extended S state model that includes misses, double-hits, inactivation, and backward-transitions, *Biophys. J. 88*, 412−421.
37. Sugiura, M., Rappaport, F., Brettel, K., Noguchi, T., Rutherford, A. W., and Boussac, A. (2004) Site-directed mutagenesis of the *Thermosynechococcus elongatus* photosystem II: The O_2-evolving enzyme lacking the redox-active tyrosine D, *Biochemistry 43*, 13549−13563.
38. Hanley, J., Deligiannakis, Y., Pascal, A., Faller, P., and Rutherford, A. W. (1999) Carotenoid oxidation in photosystem II, *Biochemistry 38*, 8189−8195.
39. Faller, P., Pascal, A., and Rutherford, A. W. (2001) β-carotene redox reactions in Photosystem II: Electron transfer pathway, *Biochemistry 40*, 6431−6440.

40. Tracewell, C. A., Cua, A., Stewart, D. H., Bocian, D. F., and Brudvig, G. W. (2001) Characterization of carotenoid and chlorophyll photooxidation in photosystem II, *Biochemistry 40*, 193−203.
41. Tracewell, C. A., Vrettos, J. S., Bautista, J. A., Frank, H. A., and Brudvig, G. W. (2001) Carotenoid photooxidation in photosystem II, *Arch. Biochem. Biophys. 385*, 61−69.
42. Bautista, J. A., Tracewell, C. A., Schlodder, E., Cunningham, F. X., Brudvig, G. W., and Diner, B. A. (2005) Construction and characterization of genetically modified *Synechocystis* sp. PCC 6803 Photosystem II core complexes containing carotenoids with shorter π-conjugation than β-carotene, *J. Biol. Chem. 280*, 38839−38850.
43. Styring, S., and Rutherford, A. W. (1987) In the oxygen-evolving complex of Photosystem II the S_0 state is oxidized to the S_1 state by D+ (Signal II_{slow}), *Biochemistry 26*, 2401−2405.
44. Peterson, S., Åhrling, K. A., and Styring, S. (1999) The EPR signals from S_0 and S_2 states of the Mn cluster in Photosystem II relax differently, *Biochemistry 38*, 15223−15230.
45. Geijer, P., Peterson, S., Åhrling, K. A., Déak, Z., and Styring, S. (2001) Comparative studies of the S_0 and S_2 multiline electron paramagnetic resonance signals from the manganese cluster in Photosystem II, *Biochim. Biophys. Acta 1503*, 83−95.
46. Kulik, L. V., Epel, B., Lubitz, W., and Messinger, J. (2005) ^{55}Mn pulse ENDOR at 34 GHz of the S_0 and S_2 states of the oxygen-evolving complex in Photosystem II, *J. Am. Chem. Soc. 127*, 2392−2393.
47. Kulik, L. V., Lubitz, W., and Messinger, J. (2005) Electron spin−lattice relaxation of the S_0 state of the oxygen-evolving complex in photosystem II and of dinuclear manganese model complexes, *Biochemistry 44*, 9368−9374.
48. Bernat, G., Morvaridi, F., Feyziyev, Y., and Styring, S. (2002) pH dependence of the four individual transitions in the catalytic S-cycle during photosynthetic oxygen evolution, *Biochemistry 41*, 5830−5843.
49. Velthuys, B. R. (1975) *Charge accumulation and recombination in system 2 of photosynthesis*, Ph.D. Thesis, University of Leiden, Leiden, The Netherlands.
50. Boussac, A., Rutherford, A. W., and Styring, S. (1990) Interaction of ammonia with the water splitting enzyme of Photosystem II, *Biochemistry 29*, 24−32.
51. Boussac, A., and Rutherford, A. W. (1990) Ca^{2+} binding to the oxygen evolving enzyme varies with the redox state of the Mn cluster, *FEBS Lett. 236*, 432−436.
52. Andreasson, L. E., and Lindberg, K. (1992) The inhibition of photosynthetic oxygen evolution by ammonia probed by EPR, *Biochim. Biophys. Acta 1100*, 177−183.
53. Kim, D. H., Britt, R. D., Klein, M. P., and Sauer, K. (1992) The manganese site of the photosynthetic oxygen-evolving complex probed by EPR spectroscopy of oriented Photosystem II membranes: The $g = 4$ and $g = 2$ multiline signals, *Biochemistry 31*, 541−547.
54. Booth, P. J., Rutherford, A. W., and Boussac, A. (1996) Location of the calcium binding site in Photosystem II: A Mn^{2+} substitution study, *Biochim. Biophys. Acta 1277*, 127−134.
55. Meulen, K. A. V., Hobson, A., and Yocum, C. F. (2004) Reconstitution of the photosystem II Ca^{2+} binding site, *Biochim. Biophys. Acta 1655*, 179−183.
56. Boussac, A. (1997) Inhomogeneity of the EPR multiline signal from the S_2 state of the photosystem II oxygen-evolving enzyme, *J. Biol. Inorg. Chem. 2*, 580−585.
57. Haumann, M., Müller, C., Liebisch, P., Iuzzolino, L., Dittmer, J., Grabolle, M., Neisius, T., Meyer-Klaucke, W., and Dau, H. (2005) Structural and oxidation state changes of the Photosystem II manganese complex in four transitions of the water oxidation cycle ($S_0 \rightarrow S_1$, $S_1 \rightarrow S_2$, $S_2 \rightarrow S_3$, and $S_{3,4} \rightarrow S_0$) characterized by X-ray absorption spectroscopy at 20 K and room temperature, *Biochemistry 44*, 1894−1908.
58. DeRose, V. J., Mukerji, I., Latimer, M. J., Yachandra, V. K., Sauer, K., and Klein, M. P. (1994) Comparison of the manganese oxygen-evolving complex in Photosystem II of spinach and *Synechococcus* sp. with multinuclear manganese model compounds by X-ray absorption spectroscopy, *J. Am. Chem. Soc. 116*, 5239−5249.
59. Yachandra, V. K., Sauer, K., and Klein, M. P. (1996) Manganese cluster in photosynthesis: Where plants oxidize water to dioxygen, *Chem. Rev. 96*, 2927−2950.
60. Robblee, J. H., Cinco, R. M., and Yachandra, V. K. (2001) X-ray spectroscopy-based structure of the Mn cluster and mechanism of photosynthetic oxygen evolution, *Biochim. Biophys. Acta 1503*, 7−23.
61. Haumann, M., Grabolle, M., Neisius, T., and Dau, H. (2002) The first room-temperature X-ray absorption spectra of higher oxidation states of the tetra-manganese complex of photosystem II, *FEBS Lett. 512*, 116−120.
62. Yano, J., Pushkar, Y., Glatzel, P., Lewis, A., Sauer, K., Messinger, J., Bergmann, U., and Yachandra, V. (2005) High-resolution Mn EXAFS of the oxygen-evolving complex in photosystem II: Structural implications for the Mn_4Ca cluster, *J. Am. Chem. Soc. 127*, 14974−14975.
63. Messinger, J., Robblee, J. H., Bergmann, U., Fernandez, C., Glatzel, P., Visser, H., Cinco, R. M., McFarlane, K. L., Bellacchio, E., Pizarro, S. A., Cramer, S. P., Sauer, K., Klein, M. P., and Yachandra, V. K. (2001) Absence of Mn-centered oxidation in the $S_2 \rightarrow S_3$ transition: Implications for the mechanism of photosynthetic water oxidation, *J. Am. Chem. Soc. 123*, 7804−7820.
64. Dau, H., Liebisch, P., and Haumann, M. (2003) X-ray absorption spectroscopy to analyze nuclear geometry and electronic structure of biological metal centers: Potential and questions examined with special focus on the tetra-nuclear manganese complex of oxygenic photosynthesis, *Anal. Bioanal. Chem. 376*, 562−583.
65. Barber, J., Ferreira, K., Maghlaoui, K., and Iwata, S. (2004) Structural model of the oxygen-evolving centre of photosystem II with mechanistic implications, *Phys. Chem. Chem. Phys. 6*, 4737−4742.
66. Ishikita, H., Saenger, W., Loll, B., Biesiadka, J., and Knapp, E.-W. (2006) Energetics of a possible proton exit pathway for water oxidation in Photosystem II, *Biochemistry 45*, 2063−2071.
67. Murray, J. W., and Barber, J. (2006) Identification of a calcium-binding site in the PsbO protein of Photosystem II, *Biochemistry 45*, 4128−4130.
68. Boussac, A., Zimmermann, J. L., Rutherford, A. W., and Lavergne, J (1990) Histidine oxidation in the oxygen-evolving Photosystem II enzyme, *Nature 347*, 303−306.
69. MacLachlan, D. J., Nugent, J. H. A., Warden, J. T., and Evans, M. C. W. (1994) Investigation of the ammonium chloride and ammonium acetate inhibition of oxygen evolution by Photosystem II, *Biochim. Biophys. Acta 1188*, 325−334.
70. Tang, X.-S., Randall, D. W., Force, D. A., Diner, B. A., and Britt, D. R. (1996) Manganese-tyrosine interaction in the Photosystem II oxygen-evolving complex, *J. Am. Chem. Soc. 118*, 7638−7639.
71. Dorlet, P., Di Valentin, M., Babcock, G. T., and McCracken, J. L. (1998) Interaction of $Y_Z^{\bullet}$ with its environment in acetate-treated Photosystem II membranes and reaction center cores, *J. Phys. Chem. B 102*, 8239−8247.
72. Lakshmi, K. V., Eaton, S. S., Eaton, G. R., Frank, H. A., and Brudvig, G. W. (1998) Analysis of dipolar and exchange interactions between manganese and Tyrosine Z in the $S_2Y_Z^{\bullet}$ state of acetate-inhibited Photosystem II via EPR spectral simulation at X- and Q-bands, *J. Phys. Chem. B 102*, 8327−8335.
73. Peloquin, J. M., Campbell, K. A., and Britt, R. D. (1998) ^{55}Mn pulsed ENDOR demonstrates that the Photosystem II "Split" EPR signal arises from a magnetically-coupled mangano-tyrosyl complex, *J. Am. Chem. Soc. 120*, 6840−6841.
74. Dorlet, P., Boussac, A., Rutherford, A. W., and Un, S. (1999) Multifrequency high-field EPR study of the interaction between the tyrosyl Z radical and the manganese cluster in plant Photosystem II, *J. Phys. Chem. B 103*, 10945−10954.
75. Dexheimer, S. L., and Klein, M. P. (1992) Detection of a paramagnetic intermediate in the S_1 state of the photosynthetic oxygen-evolving complex, *J. Am. Chem. Soc. 114*, 2821−2826.
76. Pace, R. J., Smith, P., Bramley, R., and Stehlik, D. (1991) EPR saturation and temperature-dependence studies on signals from the oxygen-evolving center of Photosystem II, *Biochim. Biophys. Acta 1058*, 161−170.
77. Hansson, Ö., Aasa, R., and Vänngård, T. (1987) The origin of the multiline and $g = 4.1$ electron paramagnetic resonance signals from the oxygen-evolving system of Photosystem II, *Biophys. J. 51*, 825−832.
78. Lorigan, G. A., and Britt, R. D. (1994) Temperature-dependent pulsed electron paramagnetic resonance studies of the S_2 State multiline signal of the photosynthetic oxygen-evolving complex, *Biochemistry 33*, 12072−12076.

79. Åhrling, K. A., Peterson, S., and Styring, S. (1998) The S_0 state EPR signal from the Mn cluster in Photosystem II arises from an isolated $S = 1/2$ ground state, *Biochemistry 37*, 8115−8120.
80. Boussac, A., Kuhl, H., Ghibaudi, E., Rögner, M., and Rutherford, A. W. (1999) Detection of an electron paramagnetic resonance signal in the S_0 state of the manganese complex of Photosystem II from *Synechococcus elongatus*, *Biochemistry 38*, 11942−11948.

BI060333U